

# On a Possibility to Determine the Sign of the Polarized Gluon Distribution

W.-D. Nowak<sup>a</sup>, A. V. Sidorov<sup>b</sup>, M.V. Tokarev<sup>c</sup>

<sup>a</sup> *DESY-IfH Zeuthen, 15735 Zeuthen, Germany*

<sup>b</sup> *Bogoliubov Laboratory of Theoretical Physics, Joint Institute for Nuclear Research,  
141980 Dubna, Moscow Region, Russia*

<sup>c</sup> *Laboratory of High Energies, Joint Institute for Nuclear Research,  
141980 Dubna, Moscow Region, Russia*

## Abstract

We investigate the possibility to draw conclusions on the sign of the spin-dependent gluon distribution,  $\Delta G(x, Q^2)$ , from existing polarized DIS data. The spin-dependent parton distributions  $\Delta u_v, \Delta d_v, \Delta \bar{u}, \Delta \bar{d}, \Delta s$ , and  $\Delta G$  are constructed in the framework of a phenomenological procedure taking into account some assumptions on signs of valence and sea parton distributions motivated by 't Hooft's mechanism of quark-quark interaction induced by instantons. The axial gluon anomaly and data on integral quark contributions to the proton spin,  $\Delta \bar{u}, \Delta \bar{d}$ , and  $\Delta \bar{s}$ , are also taken into account. Predictions for the  $x$ - and  $Q^2$ -dependencies of the polarized proton and neutron structure functions,  $g_1^p$  and  $g_1^n$ , are compared to experimental data. It is shown that the neutron structure function,  $g_1^n$ , is especially sensitive to the sign of  $\Delta G(x, Q^2)$ . The results of our analysis supports the conclusion that this sign should be positive.

# 1 Introduction

Parton distributions in the nucleon are of universal nature, hence their parametrizations obtained from deep inelastic lepton-nucleon scattering can be utilized for simulations of processes outside lepton nucleon scattering; the polarized parton distributions are especially useful to predict the behaviour of  $pp$  interactions with polarized proton beams to facilitate future research programs at the RHIC, HERA and LHC colliders.

Recent results deep inelastic lepton-nucleon scattering experiments at SLAC [1, 2] and CERN [3] on spin-dependent structure functions for proton and deuteron targets,  $g_1^p$  and  $g_1^d$ , stimulate the interest in determining the spin-dependent gluon and quark distributions in a polarized nucleon. Since a complete solution of this problem is beyond the scope of perturbative QCD and there are still no sufficiently precise non-perturbative calculations available, the usual procedure is to fit numerous parametrizations of both spin-independent and spin-dependent parton distributions to the data. Up to now there is no unique solution; the results depend in one or the other way on the method used.

Polarized parton distributions can be extracted in an indirect manner from doubly polarized deep inelastic lepton-proton and lepton-deuteron scattering; the measurable observables are the asymmetries  $A^p$  and  $A^d$ . The structure function  $g_1^p$  can be extracted from  $A^p$  according to

$$g_1^p(x, Q^2) = A^p(x, Q^2) \cdot \frac{F_2^p(x, Q^2)}{2x(1 + R(x, Q^2))}, \quad (1)$$

where additional information on the unpolarized structure function  $F_2^p$  [4] and on the ratio of longitudinal to transverse photon cross section  $R(x, Q^2) = \sigma_L/\sigma_T$  [5] are required. The deuteron structure function is determined in a similar way taking into account appropriate nuclear corrections.

Since there is no practical way at present to directly extract polarized parton distributions from experimental data it is important to develop flexible procedures to construct these distributions incorporating relevant features of the data as well as reasonable constraints derived from our present theoretical understanding of the nucleon.

At present there is no strong argument favouring a positive or negative sign of the spin-dependent gluon distribution,  $\Delta G(x, Q^2)$ . Several sets of spin-dependent parton distributions were constructed utilizing rather different approaches [6, 7, 8, 9] mostly assuming a positive sign of  $\Delta G$ . Different parameter choices leading to a different behaviour of  $\Delta G$  at  $x \rightarrow 1$  ( $G \uparrow \sim G \downarrow$ ,  $G \uparrow \gg G \downarrow$ ,  $G \uparrow \ll G \downarrow$ ) were studied in [10]. Both positive and negative values of the sign of  $\Delta G$  over a wide kinematical range  $10^{-3} < x < 1$  were considered in [9]. A detailed NLO QCD analysis of the proton and deuteron data on  $g_1$  was performed in [8] concluding that the size of the gluon distribution drives the perturbative evolution and, due to the fact that the SMC and E143 data were taken at different values of  $Q^2$ , the polarized gluon distribution turned out to be large and positive.

The aim of the present paper is to separate experimental observables being sufficiently sensitive to allow a determination of the sign of  $\Delta G$ . As we shall show later, the neutron structure function  $g_1^n$  seems to be one of those observables.

To construct the spin-dependent parton distributions a phenomenological method proposed in [9] is used. This method incorporates some constraints on shape and sign of parton distributions, it utilizes results on the quark contributions to the nucleon spin obtained in other analyses, and the effect of the axial anomaly is taken into account. We study the  $x$  and  $Q^2$  dependence of  $g_1^n(x, Q^2)$  for two different scenarios:  $\Delta G > 0$  and  $\Delta G < 0$ . The calculated predictions are compared to experimental data; a  $\chi^2$  criterion is chosen to judge in which of the two scenarios theoretical curves are better describing the experimental data on  $g_1^n(x, Q^2)$ . Eventually, the choice for a positive sign of  $\Delta G$  will turn out to be the more likely one, i.e. the polarized structure function of the neutron will be shown to be sensitive to the sign of  $\Delta G$ .

## 2 Method

The spin-dependent proton structure function  $g_1^p$  is expressed through spin-dependent parton distributions in a simple way

$$g_1^p(x, Q^2) = \frac{1}{2} \cdot \left\{ \frac{4}{9} \Delta \tilde{u}(x, Q^2) + \frac{1}{9} \Delta \tilde{d}(x, Q^2) + \frac{1}{9} \Delta \tilde{s}(x, Q^2) \right\}, \quad (2)$$

where  $\Delta q_f = q_f^+ - q_f^-$ , and the  $q_f^\pm$  are the probability distributions to find a quark having positive (+) or negative (−) helicity relatively to positive proton helicity. The neutron structure function  $g_1^n(x, Q^2)$  can be written in a similar form using the replacement  $\Delta \tilde{u} \leftrightarrow \Delta \tilde{d}$ . The valence distributions  $\Delta q_v, \Delta \bar{q}_v$  are then obtained from  $\Delta q_v = \Delta q - 2\Delta \bar{q}$ . Since in this paper we shall use the spin-dependent parton distributions constructed in [9] we briefly describe in the following sections the main features of the applied method.

### 2.1 Shape of Parton Distributions

For the general form of a spin-dependent parton distribution  $\Delta q_f$  we use

$$\Delta q_f = \text{sign}(q_f) \cdot x^{\alpha_f} \cdot (1-x)^{\beta_f} \cdot q_f, \quad q_f = u_v, d_v, \bar{u}, \bar{d}, s, G. \quad (3)$$

Here  $q_f$  is the spin-independent parton distribution,  $\alpha_f, \beta_f$  are free parameters which are to be found by comparison with experimental data. From the restriction

$$|\Delta q_f| < q_f \quad (4)$$

follows that both probability distributions  $q_f^+, q_f^-$  as well as their sum  $q_f = q_f^+ + q_f^-$  need to be positive; moreover  $\beta_f$  should not be negative. To avoid the latter constraint we introduce a renormalised parton distribution  $q_f^R = (1-x)^{\beta_f} \cdot q_f$ . This leads to the following general form of a spin-dependent parton distribution

$$\Delta q_f = \text{sign}(q_f) \cdot x^{\alpha_f} \cdot q_f^R. \quad (5)$$

We note that since all presently available procedures to construct both spin-independent and spin-dependent distributions do imply fitting procedures and have consequently no

unique solution. Hence we believe that at present it is recommended to incorporate general restrictions on  $\Delta q_f$  like the one above; this makes it easier to develop flexible schemes to construct the helicity parton distributions  $q_f^+$  and  $q_f^-$ , separately.

## 2.2 Signs of Parton Distributions

Up to now there exists neither a running experiment to directly measure the polarized gluon distribution nor does the variety of indirect analyses give a unique result. Hence there exist no strong arguments on the sign of  $\Delta G$ . Our approach will be to allow for both signs of  $\Delta G$  and compare the quality of our model-dependent predictions to the experimental data.

We note that a direct access to  $\Delta G$  will be possible in future experiments. Utilizing polarized protons at RHIC for the (approved) experiments STAR and PHENIX [11] and, possibly, for the suggested internal polarized target experiment *HERA-N* [12] at HERA, the measurement of  $\Delta G$  seems feasible in the range  $0.1 \leq x_{gluon} \leq 0.35$ . Also new doubly polarized lepton-nucleon scattering experiments proposed at CERN [13] and suggested at SLAC [14, 15] might contribute very valuable information on  $\Delta G$ .

For valence quark distributions the situation is much better defined; we take the sign of  $\Delta u_v$  as positive and that of  $\Delta d_v$  as negative, respectively. This choice is motivated by the fact that the dominant configuration in the proton wave function is  $u(\uparrow)u(\uparrow)d(\downarrow)$ , here the arrow denotes the quark spin direction. The same choice is made in most analyses of experimental data on quark contributions to the proton spin [1, 2, 3], [16]-[19].

We assume for signs of  $\Delta \bar{u}$  ( $\Delta \bar{d}$ ) to be positive (negative). This is motivated by 't Hooft's mechanism [20] for the spin configuration  $u(\uparrow)u(\uparrow)d(\downarrow)$  which determines the dynamics of quark helicity flips. The incoming left helicity quark  $q_L = (1 + \gamma_5)q/2$  scattered from zero modes in the instanton field leads to an outgoing right helicity quark  $q_R = (1 - \gamma_5)q/2$ . Effective Lagrangians are constructed in [21]; in the particular case of  $N_f = 2$  flavours it can be written as

$$L = \int d\rho \cdot n(\rho) \left( \frac{4}{3} \pi^2 \rho^3 \right)^2 \{ \bar{u}_R u_L \bar{d}_R d_L [1 + \frac{3}{32} (1 - \frac{3}{4} \sigma_{\mu\nu}^u \sigma_{\mu\nu}^d) \lambda_u^a \lambda_d^a] + (R \leftrightarrow L) \}. \quad (6)$$

Here  $\rho$  is the size of instanton,  $n(\rho)$  is the instanton density,  $\sigma_{\mu\nu} = i/4 \cdot (\gamma_\mu \gamma_\nu - \gamma_\nu \gamma_\mu)$ , and  $\lambda^a$  are matrixes for  $SU_c(3)$  group. Once the left helicity quark scatters off an instanton it becomes a right helicity one and a  $q_R \bar{q}_R$  pair is created; the helicity of the sea quarks being opposite to that of the initial quark. In other words, the spin flip of the valence quarks  $u^+$  and  $d^-$  determines the sign of the corresponding sea quark distributions - negative for  $\Delta \bar{d}$  and positive for  $\Delta \bar{u}$ . A negative sign of  $\Delta s$  is in agreement with the arguments mentioned above and is supported by the results of several analyses of  $g_1^p$  data [1, 2, 3], [16]-[19].

## 2.3 Inclusion of Axial Anomaly

It was shown in [22] that the flavour-singlet axial current

$$A_\mu^0 = \sum_{f=u,d,s} \bar{q}_f \gamma_\mu \gamma_5 q_f \quad (7)$$

diverges at the quark level due to the one-loop triangle anomaly

$$\partial^\mu A_\mu = \frac{\alpha_s}{\pi} \cdot N_f \cdot \text{tr}\{F_{\mu\nu}\tilde{F}^{\mu\nu}\}, \quad (8)$$

where  $\tilde{F}_{\mu\nu} = \epsilon_{\mu\nu\beta\gamma}F^{\beta\gamma}$ ,  $F_{\mu\nu} = \partial_\mu A_\nu - \partial_\nu A_\mu + [A_\mu A_\nu]$ ,  $A_\mu = A_\mu^a \cdot \lambda^a$ ,  $\alpha_s$  is the strong coupling constant, and  $N_f$  is the number of flavours. The anomaly induces a mixing between the gluon and the flavour singlet axial current of quarks. For this reason, the helicity carried by each flavour undergoes a renormalization

$$\Delta\tilde{q}_f(x, Q^2) = \Delta q_f(x, Q^2) - \frac{\alpha_s(Q^2)}{2\pi} \cdot \Delta G(x, Q^2). \quad (9)$$

It was suggested in [22] that the axial anomaly might play a key role and modify the naive quark model predictions; hence parton distributions will presumably become much more sensitive to the sign of the polarized gluon distribution. Consequently, the spin-dependent structure functions  $g_1^p$  and  $g_1^n$  would become more sensitive to  $\Delta G$ , as well.

## 2.4 Integral Parton Contributions to the Proton Spin

A further input required to our analysis is the total contribution of each quark species to the proton spin. We utilize the results of a recent analysis [23] of the structure functions  $g_1^p$  and  $g_1^d$  from SMC and SLAC data incorporating  $3^{rd}$  order pQCD corrections to the Bjorken sum rule. The relative quark contributions to the proton spin were determined as  $\Delta\tilde{u} = 0.83 \pm 0.03$ ,  $\Delta\tilde{d} = -0.43 \pm 0.03$ ,  $\Delta\tilde{s} = -0.10 \pm 0.03$  at a renormalization scale  $Q_0^2 = 10 \text{ (GeV/c)}^2$ . Using these values and the definition

$$\int_0^1 \Delta\tilde{q}_f(x, Q_0^2) dx = \Delta\tilde{f}, \quad f = u, d, s \quad (10)$$

the free parameters  $\alpha_f, \beta_f$  in the parametrization of our spin-dependent parton distributions  $\Delta u_V, \Delta d_V, \Delta\bar{u}, \Delta\bar{d}, \Delta s, \Delta G$  were determined in [9].

## 3 Results and Discussion

In fig. 1 (a,b) and 2 (a,b) the  $x$ -dependence of  $g_1^p$  and  $g_1^n$  is shown for different parametrizations of parton distributions constructed with  $\Delta G > 0$  (a) and  $\Delta G < 0$  (b). The dashed, solid and dotted lines correspond to the parameters  $\alpha_f, \beta_f$  taken from Table 1-3 and 4-6 of Ref. [9], respectively.

From fig. 1 (a,b) is seen that all theoretical curves for the *proton* structure function  $g_1^p$  are in reasonable agreement with experimental data [1, 16, 19], i.e. there seems to be no apparent sensitivity to the sign of  $\Delta G$ . In contrast, from fig. 2 (a,b), displaying experimental data and theoretical curves for the *neutron* structure function  $xg_1^n$ , one can deduce a certain dependence of the theoretical curves on the sign of  $\Delta G$  in the range  $0.1 < x < 0.3$ . Hence there is some hope that  $xg_1^n$  exhibits a certain sensitivity to the sign of  $\Delta G$ .

Fig. 3 (a,b) shows the  $x$ -dependence of the *proton* structure function  $xg_1^p(x, Q^2)$  at different values of four-momentum transfer,  $Q^2 = 1, 10, 100$  (GeV/c)<sup>2</sup>. The  $Q^2$  behaviour of  $xg_1^p$  appears qualitatively different for  $\Delta G > 0$  and  $\Delta G < 0$ , respectively. In the first case the maximum of the curve is moved to lower  $x$  with increasing  $Q^2$ , in the second one the position of the maximum is not affected. If  $\Delta G > 0$  the prediction *increases* with  $Q^2$  for  $x < 0.01$ . If  $\Delta G < 0$ , the prediction *decreases* with  $Q^2$  over the full  $x$ -range.

Fig. 4 (a,b) displays the  $x$ -dependence of the *neutron* structure function  $xg_1^n(x, Q^2)$  in the same fashion, i.e. for  $Q^2 = 1, 10$  (GeV/c)<sup>2</sup>. If  $\Delta G > 0$  the differences for different  $Q^2$  appear mainly at very low  $x$ -values and, in addition, at moderate  $x \simeq 0.3$ . This sensitivity to the sign of  $\Delta G$  is too weak for present experimental errors, however, it might be used later when more precise data on  $g_1^n(x, Q^2)$  should become available. For  $\Delta G < 0$  one observes a rather strong  $Q^2$ -dependence at lower  $x$ -values and a somewhat characteristic dip at higher  $x$ , its position being almost independent on  $Q^2$ .

To be closer to the presently available  $Q^2$ -values we show in fig. 5 the  $x$ -dependence of  $xg_1^n(x, Q^2)$  at  $Q^2 = 1, 3, 5, 10$  (GeV/c)<sup>2</sup> together with the presently available experimental data. (Due to the experimental errors the different ordinate is chosen in fig. 5(d) than in fig. 5(a,b,c).) The behaviour of  $xg_1^n$  on  $Q^2$  is qualitatively and quantitatively different for the two scenarios  $\Delta G > 0$  and  $\Delta G < 0$ , especially at low  $Q^2$ . Apparently, in the range  $x < 0.1$  the experimental data on  $g_1^n$  at  $Q^2 < 10$  (GeV/c)<sup>2</sup> should be able to discriminate between positive and negative sign of the polarized gluon distribution.

We apply a  $\chi^2$  criterion to quantitatively distinguish between the two scenarios by comparing our constructed parton distributions to the experimental data sets from SLAC and CERN [2, 3, 18]. The obtained results are summarized in Table 1. There the references for experimental data on  $g_1^n$ , the average  $Q^2$  values, and the number of experimental points are shown in column 1, 2, and 3, respectively. The 'all' in col. 2 takes into account that each individual experimental point was measured at another average  $Q^2$ , i.e. here the  $\chi^2$  is calculated using in the theoretical calculation the correct average  $Q^2$ -value at each  $x$ -point. The corresponding kinematically accessible ranges are  $1.1 \div 5.2$  (GeV/c)<sup>2</sup> for E142 and  $1.3 \div 48.7$  (GeV/c)<sup>2</sup> for SMC. This method seems to us the closest possible description of the data by a theoretical calculation, hence we expect the  $\chi^2$  values obtained for the 'all' comparison to yield the best possible separation.

Experiment	$\langle Q^2 \rangle$ (GeV/c) <sup>2</sup>	data points	$\chi^2$ / ndf $\Delta G > 0$	$\chi^2$ / ndf $\Delta G < 0$
E142 [18]	2	8	1.20	2.05
E143 [2]	3	9	0.89	1.41
SMC [3]	10	12	1.28	1.63
HERMES [24]	3	8	0.86	1.20
E142 [18]	all	8	1.45	2.30
SMC [3]	all	12	1.35	2.41

Table 1.  $\chi^2$  comparison between theoretical predictions, calculated for the two scenarios  $\Delta G > 0$  and  $\Delta G < 0$ , and experimental data on  $g_1^n(x, Q^2)$ .

From table 1 one can see that for every data set the  $\chi^2$  per degree of freedom is significantly better in the case  $\Delta G > 0$  compared to the case  $\Delta G < 0$ . These results can be considered as clear quantitative evidence that the case  $\Delta G > 0$  is the more likely scenario compared to the case  $\Delta G < 0$ .

We note that our result supports the conclusion on a positive sign of  $\Delta G > 0$  obtained recently by a NLO QCD fit to  $g_1$  proton and deuteron data [8].

Finally we present in table 2 our results for the integral quark –  $\Delta\Sigma$  – and gluon –  $\Delta g$  – contributions to the proton spin calculated with the low limit  $x_{min} = 10^{-3}$ . Whereas in the more likely scenario  $\Delta G > 0$  the quark contribution  $\Delta\Sigma$  appears to be almost stable with  $Q^2$  it drops by almost a factor of 2 when increasing  $Q^2$  from 3 to 10  $(\text{GeV}/c)^2$  in the less likely case  $\Delta G < 0$ . In both scenarios  $\Delta g$  rises by about 10% within the same  $Q^2$  range.

$Q_0^2$ $(\text{GeV}/c)^2$	$\Delta\Sigma$		$\Delta g$	
	$\Delta G > 0$	$\Delta G < 0$	$\Delta G > 0$	$\Delta G < 0$
3	0.290	0.520	1.78	-3.01
5	0.293	0.420	1.86	-3.20
10	0.298	0.296	1.95	-3.41

Table 2. Integral quark –  $\Delta\Sigma$  – and gluon –  $\Delta g$  – contributions to the proton spin, calculated from the constructed polarized parton distribution functions for the two scenarios  $\Delta G > 0$  and  $\Delta G < 0$ .

## 4 Conclusions

The possibility to draw conclusions on a positive or negative sign of the polarized gluon distribution  $\Delta G(x, Q^2)$  was studied using a phenomenological procedure to construct spin-dependent parton distributions. The method includes some constraints on the signs of valence and sea quark distributions, takes into account the axial gluon anomaly and utilizes results on integral contributions to the nucleon spin,  $\Delta\tilde{u}, \Delta\tilde{d}, \Delta\tilde{s}$ . Investigating the  $x$ - and  $Q^2$ -dependencies of the structure functions  $g_1^p$  and  $g_1^n$  constructed by this method we introduce a  $\chi^2$  criterion to discriminate between the two scenarios obtained for  $\Delta G > 0$  and  $\Delta G < 0$ , respectively. The neutron structure function turned out to be sufficiently sensitive to the sign of  $\Delta G(x, Q^2)$ , even at the present level of only moderate experimental errors. The results of our analysis strongly support the conclusion that the sign of  $\Delta G(x, Q^2)$  is positive. New data on the neutron structure function  $g_1^n$  from the latest SLAC experiments and from HERMES at DESY will undoubtedly allow to draw a more definite conclusion on the sign of the polarized gluon distribution.

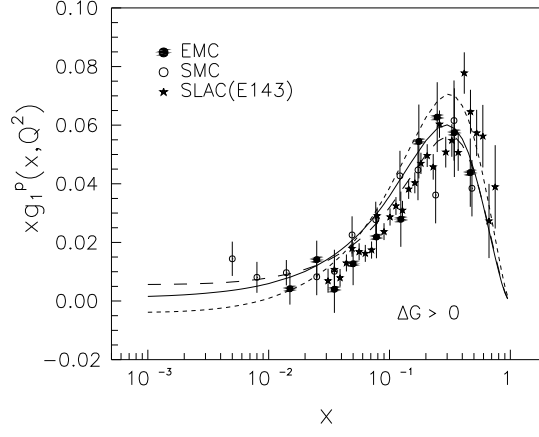
## Acknowledgements

This work was partially supported by Grants of the Heisenberg-Landau Program for 1996 and of the Russian Foundation of Fundamental Research under No. 95-02-05061 and No. 96-02-18897.

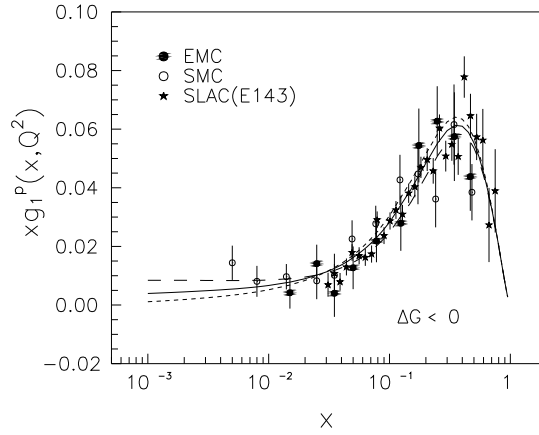
## References

- [1] K.Abe et al., *Phys. Rev. Lett.* **74** (1995) 346.
- [2] K. Abe et al., *Phys. Rev. Lett.* **75** (1995) 25.
- [3] D.Adams et al., *Phys. Lett.* **B357** (1995) 248.
- [4] M.Arneodo et al., *Phys. Lett.* **B364** (1995) 107;  
T.Ahmed et al., *Nucl. Phys.* **B439** (1995) 471;  
M.Derrick et al., *Z.Phys.* **C65** (1995) 379.
- [5] L.Whitlow et al., *Phys. Lett.* **B250** (1990) 193.
- [6] S.J. Brodsky, M. Burkardt, I.Schmidt, *Nucl.Phys.* **B273** (1995) 197.
- [7] M. Glück, E.Reya, W. Vogelsang, *Phys. Lett.* **B359** (1995) 210.
- [8] R.D.Ball, S. Forte, G.Ridolfi, Preprint CERN-TH/95-266, 1995.
- [9] M.V. Tokarev, JINR Preprint E2-96-304, Dubna, 1996.
- [10] T. Gehrmann, W.J.Stirling, *Z.Phys.* **C65** (1995) 461.
- [11] The RHIC Spin Collaboration, RHIC Spin Physics Proposal, (BNL, Upton, NY, Sept. 1993).
- [12] W.-D. Nowak, DESY 96-095, hep-ph/9605411, to be publ. in the Proc. of the Adriatico Research Conference "*Trends in Collider Spin Physics*", ICTP Trieste, Dec. 4-8, 1995.
- [13] The COMPASS Collaboration, Proposal for Common Muon and Proton Apparatus for Structure and Spectroscopy. CERN/SPSLC/96-14, SPSLC/P297, March 1, 1996.
- [14] V. Breton, talk at the 'Journee du Spin', CE Saclay, January 1995
- [15] P.Bosted, talk at the 'SLUO Meeting', Stanford, 1996
- [16] J.Ashman, et al., *Phys. Lett.* **B206** (1988) 210; *Nucl. Phys.* **B328** (1989) 1.
- [17] B. Adeva et al., *Phys. Lett.* **B302** (1993) 533.
- [18] P.L. Anthony et al., *Phys. Rev. Lett.* **71** (1993) 959;  
The E142 Collaboration, F. Staley et al., In: Proc. International Europhysics Conf. on High Energy Physics, HEP93, Marseille, France, 22-28 July, 1994, p.114.
- [19] D.Adams et al., *Phys. Lett.* **B329** (1994) 399.
- [20] G.'t Hooft, *Phys. Rev.* **D14** (1976) 3432.
- [21] M.A.Shifman, A.I. Vainshtein, V.I. Zakharov, *Nucl.Phys.* **B163** (1980) 46.
- [22] A.V. Efremov, O.V. Teryaev, Dubna report E2-88-287, 1988;  
G. Altarelli, G.G. Ross, *Phys. Lett.* **B212** (1988) 391.
- [23] J.Ellis, M.Karliner, Preprint CERN-TH. 7324/94, 1994.
- [24] M. Vetterli for the HERMES Collaboration, talk at the 'Workshop on Deep Inelastic Scattering', Rome, April 1996.
- [25] M.Glück, E.Reya, A.Vogt, *Z.Phys.* **C48** (1990) 471.



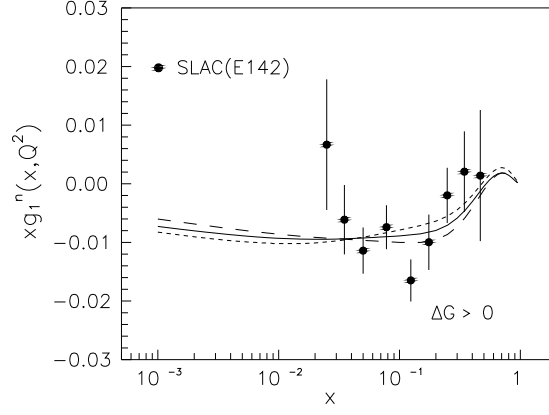


a)

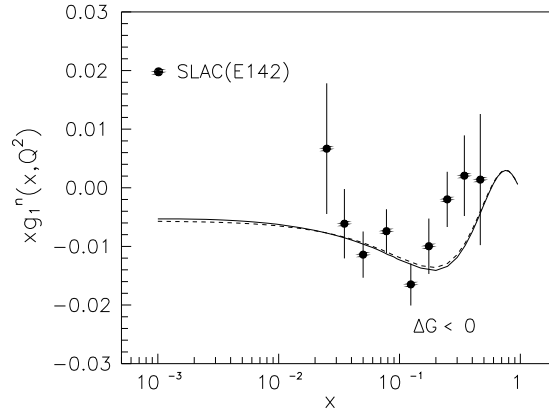


b)

**Figure 1.** Deep-inelastic proton structure function  $xg_1^p(x, Q^2)$ . Experimental data:  $\star$  - [1],  $\bullet$  - [16],  $\circ$  - [19]. Theoretical curves: (a) -  $\Delta G > 0$  and (b) -  $\Delta G < 0$  at  $Q^2 = 10 \text{ (GeV/c)}^2$ . Parametrizations of parton distributions:  $---$ ,  $—$ ,  $- \cdot -$  are taken from Tables 1-3 and Tables 4-6 [9], respectively.

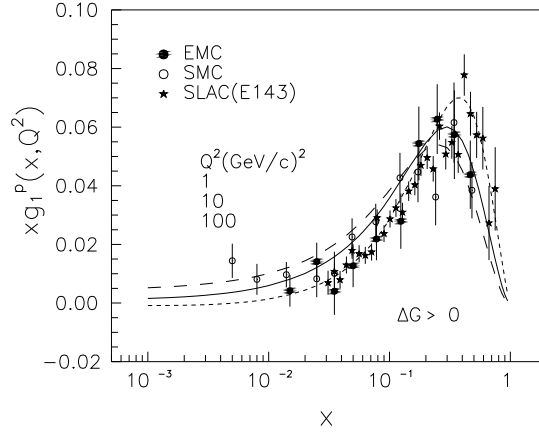


a)

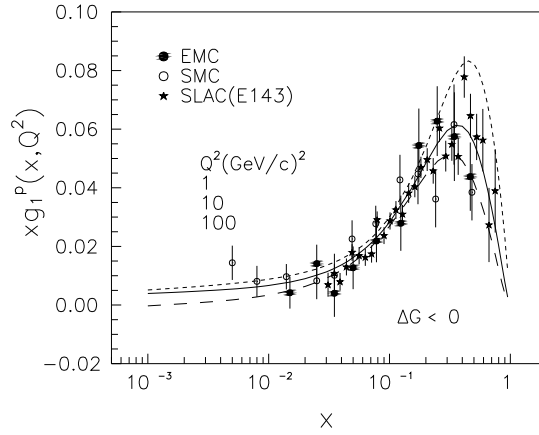


b)

**Figure 2.** Deep-inelastic neutron structure function  $xg_1^n(x, Q^2)$ . Experimental data: • - [18]. Theoretical curves: (a) -  $\Delta G > 0$  and (b) -  $\Delta G < 0$  at  $Q^2 = 10 \text{ (GeV/c)}^2$ . Parametrizations of parton distributions: ---, —, — — are taken from Tables 1-3 and Tables 4-6 [9], respectively.

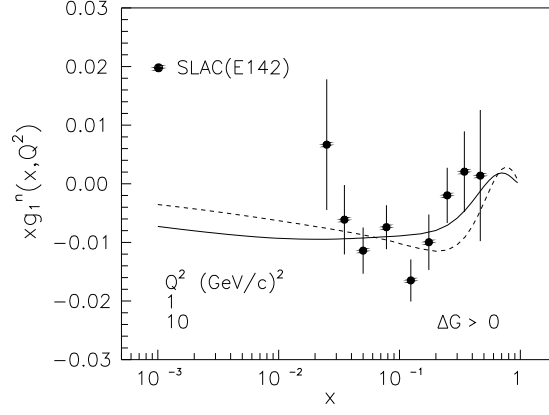


a)

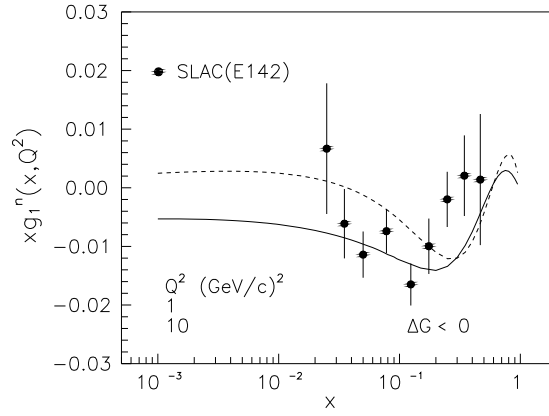


b)

**Figure 3.** Deep-inelastic proton structure function  $xg_1^p(x, Q^2)$ . Experimental data:  $\star$  - [1],  $\bullet$  - [16],  $\circ$  - [19]. Theoretical curves: (a) -  $\Delta G > 0$ , (b) -  $\Delta G < 0$  and  $---$  -  $1 \text{ (GeV/c)}^2$ ,  $---$  -  $10 \text{ (GeV/c)}^2$ ,  $---$  -  $100 \text{ (GeV/c)}^2$ . Parametrizations of parton distributions are taken from Tables 2 and 5 [9].

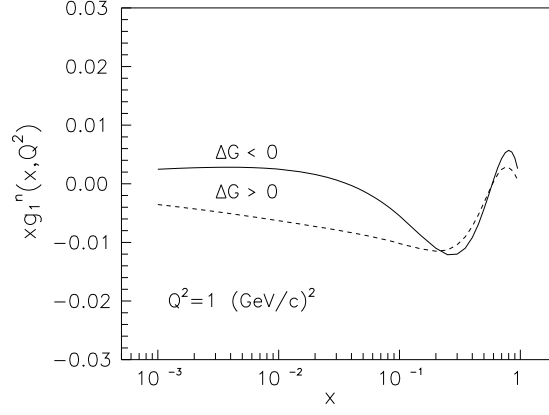


a)

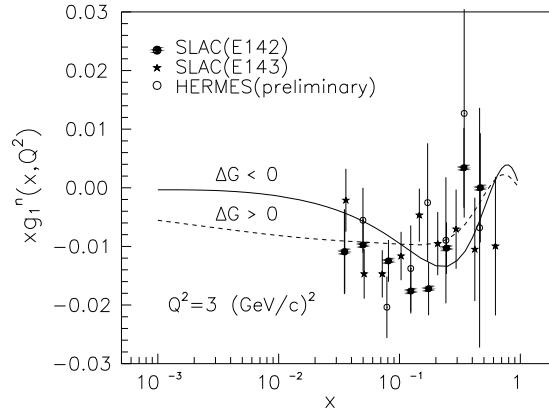


b)

**Figure 4.** Deep-inelastic neutron structure function  $xg_1^n$ . Experimental data:  $\bullet$  - [18]. Theoretical curves: (a) -  $\Delta G > 0$ , (b) -  $\Delta G < 0$  and  $---$  -  $1 \text{ (GeV/c)}^2$ ,  $---$  -  $10 \text{ (GeV/c)}^2$ . Parametrizations of parton distributions are taken from Tables 2 and 5 [9].

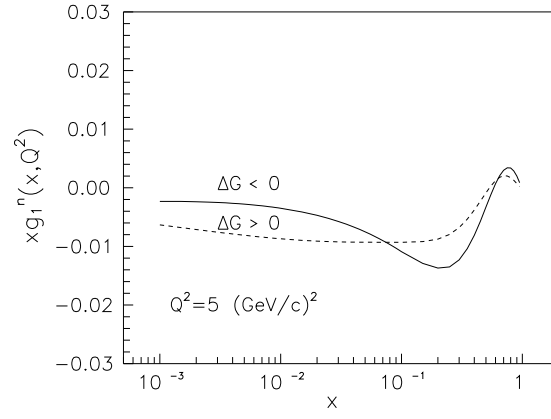


a)

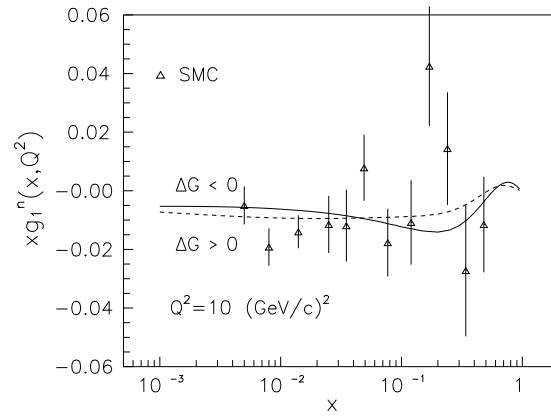


b)

**Figure 5.** Deep-inelastic neutron structure function  $xg_1^n(x, Q^2)$ . Experimental data:  $\star$  - [2],  $\triangle$  - [3],  $\bullet$  - [18],  $\circ$  - [24]. Theoretical curves:  $---$  -  $\Delta G > 0$ ,  $---$  -  $\Delta G < 0$  at  $Q^2 = 1, 3, 5, 10 \text{ (GeV/c)}^2$ . Parametrizations of parton distributions are taken from Tables 2 and 5 [9].



c)



d)

**Figure 5.** Continued